How to cite: Angew. Chem. Int. Ed. 2020, 59, 15008–15013
International Edition: doi.org/10.1002/anie.202005449
German Edition: doi.org/10.1002/ange.202005449

Fullerenes

Studying Natural Buckyballs and Buckybowls in Fossil Materials

*Zahra Farmani, Alessandro Vetere, Corentin Poidevin, Alexander A. Auer, and Wolfgang Schrader**

In memory of Professor Walter Thiel

Abstract: *Buckyballs (fullerenes) were first reported over 30 years ago, but still little is known regarding their natural occurrence, since they have so far only been found at sites of high-energy incidents, such as lightning strikes or meteor impacts, but have not been reported in low-energy materials like fossil fuels. Using ultrahigh-resolution mass spectrometry, a wide range of fullerenes from C_{30} to C_{114} was detected in the asphaltene fraction of a heavy crude oil, together with their building blocks of $C_{10n}H_{10}$ stoichiometry. High-level DLPNO-CCSD(T) calculations corroborate their stability as spherical and hemispherical species. Interestingly, the maximum intensity of the fullerenes was found at C_{40} instead of the major fullerene C_{60}. Hence, experimental evidence supported by calculations show the existence of not only buckyballs but also buckybowls as 3-dimensional polyaromatic compounds in fossil materials.*

Introduction

Buckyballs (fullerenes) have only been known since the first theoretical reports from Osawa[1] and were first synthesized by Curl, Kroto, and Smalley using a laser experiment.[2] The late discovery of natural fullerenes is linked to the absence of sophisticated detection methods and their low abundance in the earth's crust,[3] which led them to be largely ignored. The presence of fullerenes in natural environmental compartments is often related to a high-energy incident, such as meteor impact, lightning strike, or other events.[4] Therefore, our knowledge of the natural occurrence of fullerenes is limited and they have not been reported yet for low-energy surroundings.[5]

Among the most abundant sources of organic carbon in natural surroundings are fossil materials, for example, fossil fuels. Here, a very large number of different hydrocarbon compounds is found. Reports indicate that the number of individual chemical compounds exceeds one million in a crude oil.[6] The different constituents of crude oil, especially heavy aromatic compounds, have so far mostly been thought of as being formed from graphitic-type compounds, that is, having planar structures.

During the last decades, the composition of available crude oils has changed, as the light and sweet crudes have been diminished and more often heavy and sour resources need to be upgraded. That has led to a higher emphasis on the investigation of the heaviest part of crude oil, known as the asphaltene fraction. Asphaltenes are by definition the part that is insoluble in paraffinic solvents (*n*-pentane or *n*-heptane) but soluble in toluene. They contain compounds with the highest amounts of heteroelements and larger aromatic cores than other parts of crude oil.[7]

The only way to get any molecular information for such complex mixtures is the use of ultrahigh-resolution mass spectrometry (UHRMS), which allows separation of the major mass splits up to the mass of an electron.[7b,8] While complex samples have the tendency to cause suppression and discrimination effects[8c,9] this is still the only analytical method that makes it possible to simultaneously detect hundreds of thousands of individual molecular compositions.[10]

However, the major drawback is the fact that mass spectrometry (MS), while highly accurate, only offers elemental compositions of unknown compounds. Structural details can only be gained by fragmentation studies using collision-induced dissociation (CID).[11] However, different structural isomers cannot be differentiated by MS alone. Therefore, we have added computational methods using high-level coupled cluster calculations to better understand the different chemical structures.

Results and Discussion

Soft ionization methods for mass spectrometry lead to the formation of molecular ions only, and no changes to the initial samples occur. While laser-based ionization has been suspected to form molecules such as fullerenes during the ionization process,[12] electrospray ionization is known as a very soft ionization method.[13]

It has been shown that during the electrospray-ionization process, cluster ions can be formed. However, the method is interesting for the ionization of polyaromatic compounds, because radical ions are formed in the electrochemical cell of the nebulizer and no interfering reactions can occur due to the low ionization energies.[14] Still, when we studied a very complex asphaltene sample of a heavy crude oil, the results

[*] M. Sc. Z. Farmani, Dr. A. Vetere, Dr. C. Poidevin, Prof. Dr. A. A. Auer, Prof. Dr. W. Schrader
Max-Planck-Institut für Kohlenforschung
Kaiser-Wilhelm-Platz 1, 45470 Mülheim an der Ruhr (Germany)
E-mail: wschrader@mpi-muelheim.mpg.de

Supporting information and the ORCID identification number(s) for the author(s) of this article can be found under: https://doi.org/10.1002/anie.202005449.

© 2020 The Authors. Published by Wiley-VCH Verlag GmbH & Co. KGaA. This is an open access article under the terms of the Creative Commons Attribution Non-Commercial License, which permits use, distribution and reproduction in any medium, provided the original work is properly cited, and is not used for commercial purposes.

were very surprising, since the major signals corresponded to the radical cations of pure-carbon compounds, ranging from C_{30} up until C_{114} (see Figure 1 and Figure 2).

From a chemical point of view, these carbon-only compounds can only correlate to either buckyballs (fullerenes) or open-ended graphene sheets. The latter seems improbable because the edges of the sheets would be terminated either by reactive carbenes, or by other elements, which are detectable. Here, the signals resulted from carbon-only compounds, with fullerenes being the most probable.

To verify that the detected compounds are indeed fullerenes, CID studies were carried out. As a reference, standard buckminsterfullerene (C_{60}) was used (see Figure 3). The CID spectra show a very characteristic fragmentation pattern of C_2 losses, but only at very high collision energies. Usually, organic compounds can be fragmented at collision energies between 10–60 eV. Here, to achieve fragmentation of the precursor ions, the fragmentation energies had to be set to more than 200 eV for both the fullerene standard and the

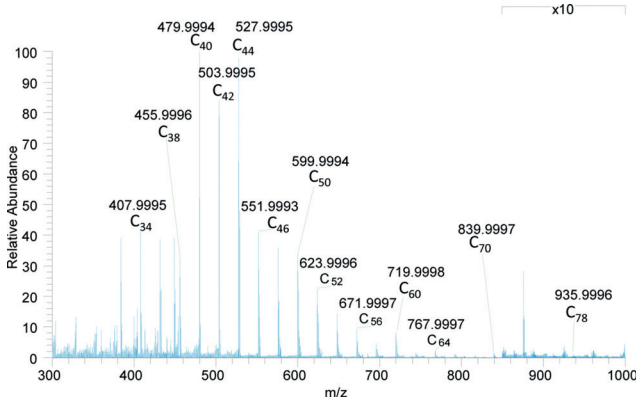

Figure 1. Electrospray mass spectrum of an asphaltene fraction (*m/z* 300–1000). The major signals can be attributed to compounds that only contain carbon (intensity scale is zoomed in the higher mass range).

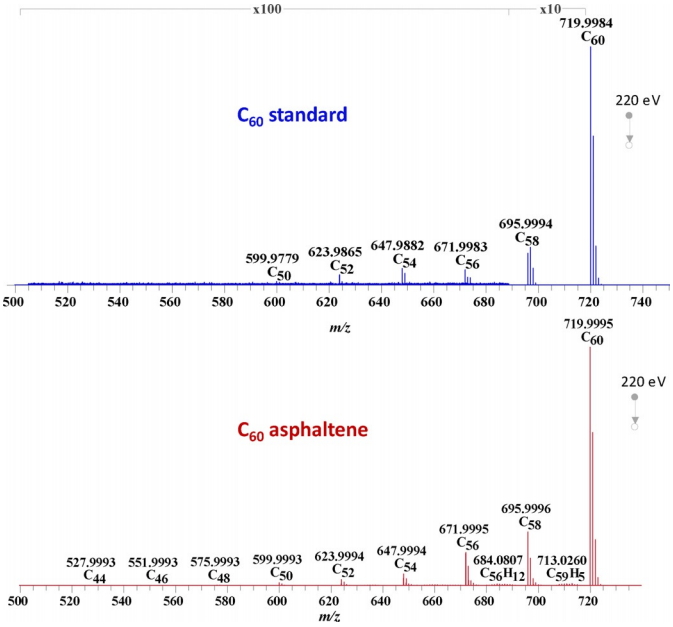

Figure 3. The two spectra show results from CID-fragmentation studies, presenting the results of a C_{60} standard and the fragmentation of the ion corresponding to C_{60} from the asphaltene fraction. Comparison of the two spectra reveals the same fragmentation pattern, which is also true for all other CID spectra that were measured. The data were obtained at collision energies above 200 eV. Additional examples are documented in Figure S1. Part of spectrum is zoomed-in as noted.

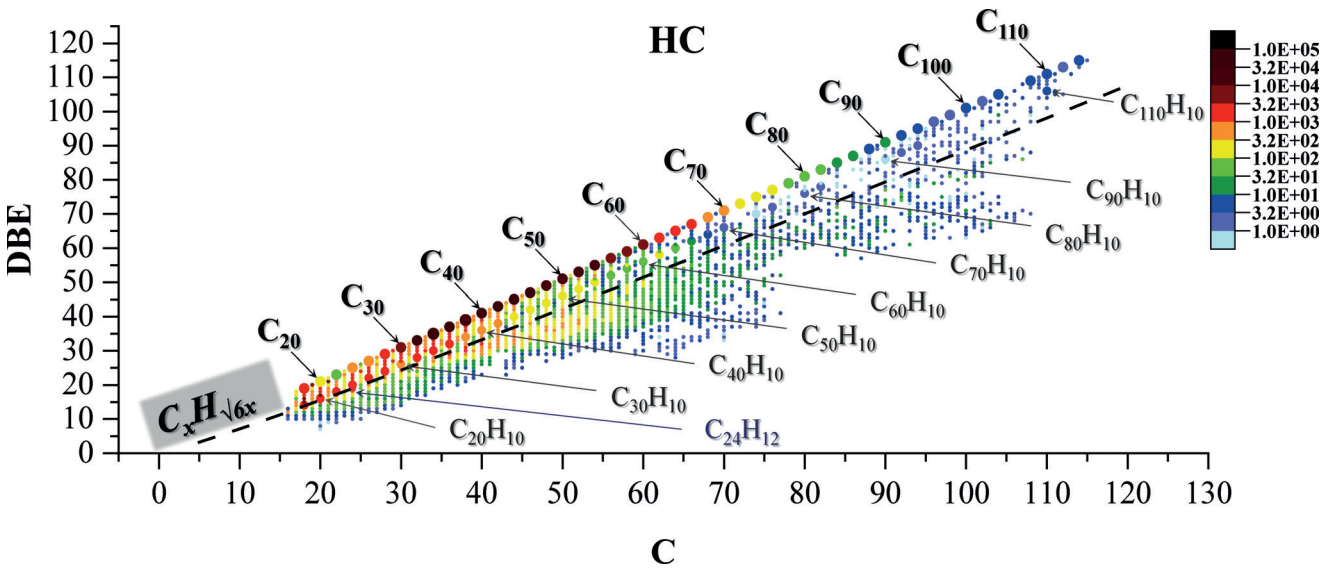

Figure 2. Kendrick plot of the hydrocarbon class obtained from the ESI-MS spectrum, showing all hydrocarbon compounds detected, indicating the broad window of carbon-only compounds ranging from C_{30} to C_{114} (highlighted by larger dots). Additional highlighted compounds are the corresponding building blocks (buckybowls) from $C_{20}H_{10}$ to $C_{110}H_{10}$. The dashed line represents the border of the real planar limit for aromatic cores: compounds detected above are considered to be non-planar, compounds below the line can exhibit either planar or non-planar cores (depending on the distribution of carbon atoms between the core structure and aliphatic side chains).

 © 2020 The Authors. Published by Wiley-VCH Verlag GmbH & Co. KGaA, Weinheim

asphaltene sample, thus indicating a very stable and condensed ion such as a spherical fullerene. In addition to the C_{60} standard, a number of different fullerene signals from the asphaltene sample were fragmented (see Figure S1 in the Supporting Information).The results from the asphaltene C_{60} are also presented in Figure 3 and show a comparable fragment spectrum as the buckminsterfullerene standard.

All precursor ions behaved similarly and the spectra show a comparable fragmentation pattern, where always a series of C_2 losses are detected. This is in agreement with earlier studies about the fragmentation of fullerenes. They only fragment at high collision energies,[15] where often a sector-field mass spectrometer was used that allows high-energy collisions, and show the distinct even-numbered carbon loss, which is most likely forming the most stable fragment ion. This verifies that a wide range of naturally occurring fullerenes is present in fossil materials, which have been formed under geological conditions.

In addition to the fullerenes, a wide range of different polyaromatic hydrocarbons are present in crude-oil asphaltenes. The overall number of peaks detected here exceeds 50000, from which roughly 4000 can be assigned as pure hydrocarbons, while others have at least one heteroatom in the molecule. Most of these hydrocarbons have a structure where an aromatic core is connected with one or more additional aliphatic side chains. The different elemental compositions are summarized in a Kendrick plot (Figure 2) where the DBE value represents the number of double bonds and ring-closing bonds, which is an indication about the aromaticity. While next to the fullerenes a large number of different hydrocarbons are detected, some stand out in regard to fullerenes. Therefore, another series exhibiting the chemical formula of $C_{10n}H_{10}$ is emphasized here because they appear as potential building blocks of fullerenes. Figure 4 A shows a set of different mass windows indicating a series of hydrogen-deficient compounds consisting of different numbers of carbon atoms together with 10 hydrogen atoms representing the compounds with $C_{10n}H_{10}$ stoichiometry (examples with $n = 2$–6 are emphasized here as examples). The limitation of the hydrogen/carbon ratio does not allow a wide variety of realistic structures. Some examples are displayed in Figure 4 B and C. Unfortunately, mass spectral data can only reveal the elemental composition but not the structure of such a compound. Therefore, we studied potential structures using electronic structure theory at the highest level of theory available for such systems to date: a combination of density functional theory methods and coupled-cluster single-point energies.[16]

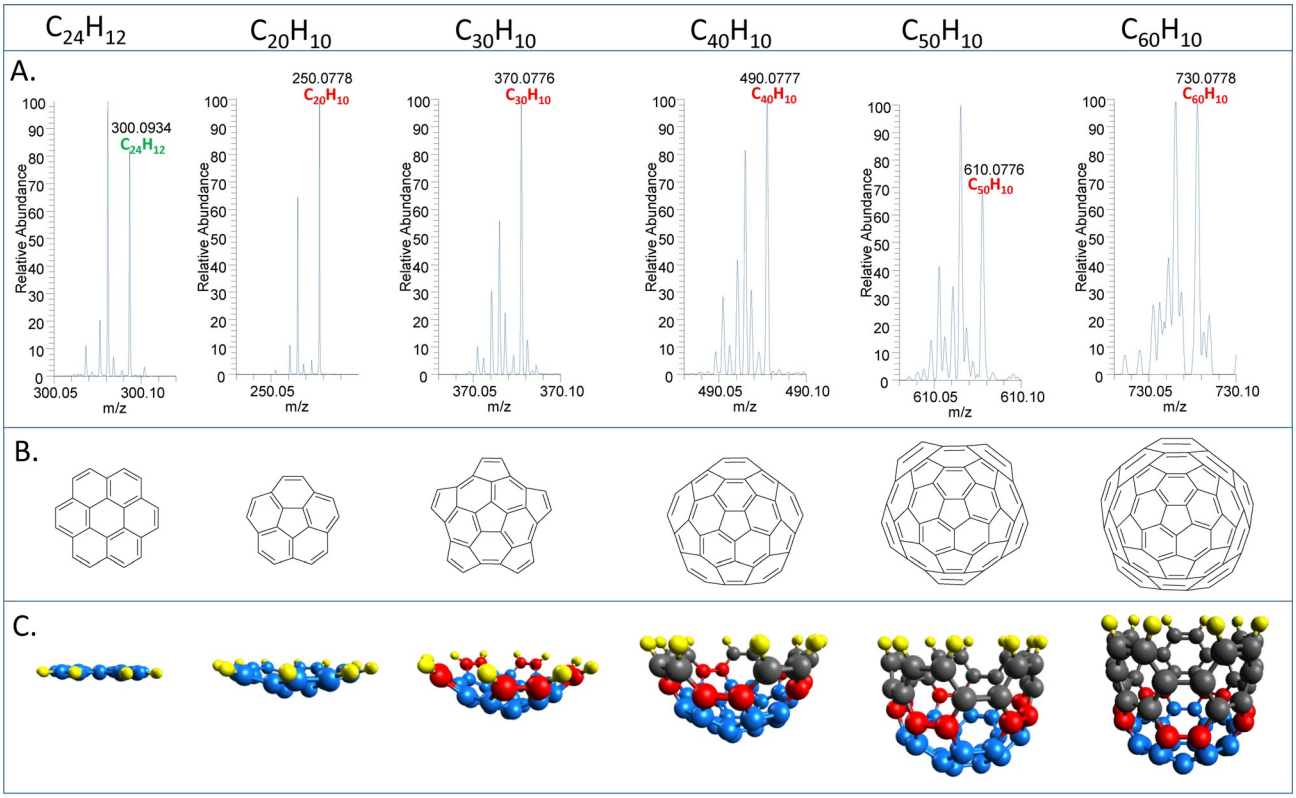

Figure 4. A) A set of mass spectra excerpts showing signals of a series of compounds with a formula of $C_{10n}H_{10}$, which are considered building blocks of fullerenes. B) The most promising example structures are shown as a two-dimensional representation of fullerene building blocks. C) While coronene ($C_{24}H_{12}$), consisting of one central 6-membered ring that is surrounded by six 6-membered rings, is a flat, graphitic structure, when a 5-membered ring is introduced, the structure of the molecule starts to fold into a sphere. Corannulene ($C_{20}H_{10}$) is the first member of this group. The bending and bowl-type structure increases with size as can be seen at the bottom, where sketches of the corresponding optimized geometries are shown. The blue carbon atoms refer to corannulene, and adding the red carbon atoms make it a C_{30} endcap. The carbon atoms in grey show a tubular extension of 6-membered rings, which expand the size of the molecule. Open ends are then terminated by hydrogen atoms, shown in yellow.

 © 2020 The Authors. Published by Wiley-VCH Verlag GmbH & Co. KGaA, Weinheim

While the structural chemical space for a given stoichiometry is rather large, this study is aimed at determining the relative thermodynamic stability of several structural patterns, based on our chemical knowledge of polycyclic aromatic hydrocarbons. Within the series of $C_{10n}H_{10}$ compounds, which were accurately observed by MS, a broad variety of structures were considered, including several defective, planar structures, as well as structures that are bent or represent small carbon tubes (see Figure 5 and additional data in Figures S2–S6 in the Supporting Information). Note that for most stoichiometries, it is not possible to construct flat structures that are composed of only 6-membered aromatic rings without including defects, for example, missing hydrogen terminations. 5-membered ring(s) can also be included, leading to bowl like structures for small n values and to amphore-like compounds (resembling an endcapped nanotube) for larger n values. The different types of structural patterns that are theoretically considered are summarized in Table 1. The first major feature we found when studying the $C_{10n}H_{10}$ series is that for every stoichiometry, the lowest-energy structure is the one that has the maximum number of aromatic 6-membered rings (ARs). This can already be seen in the $C_{20}H_{10}$ series, where the bowl structure B1 has five ARs, and the lowest-energy planar structure found (P1) only has 4, as shown in Figure 5 A. However, the energy difference between these two isomers (164 kJ mol^{-1})

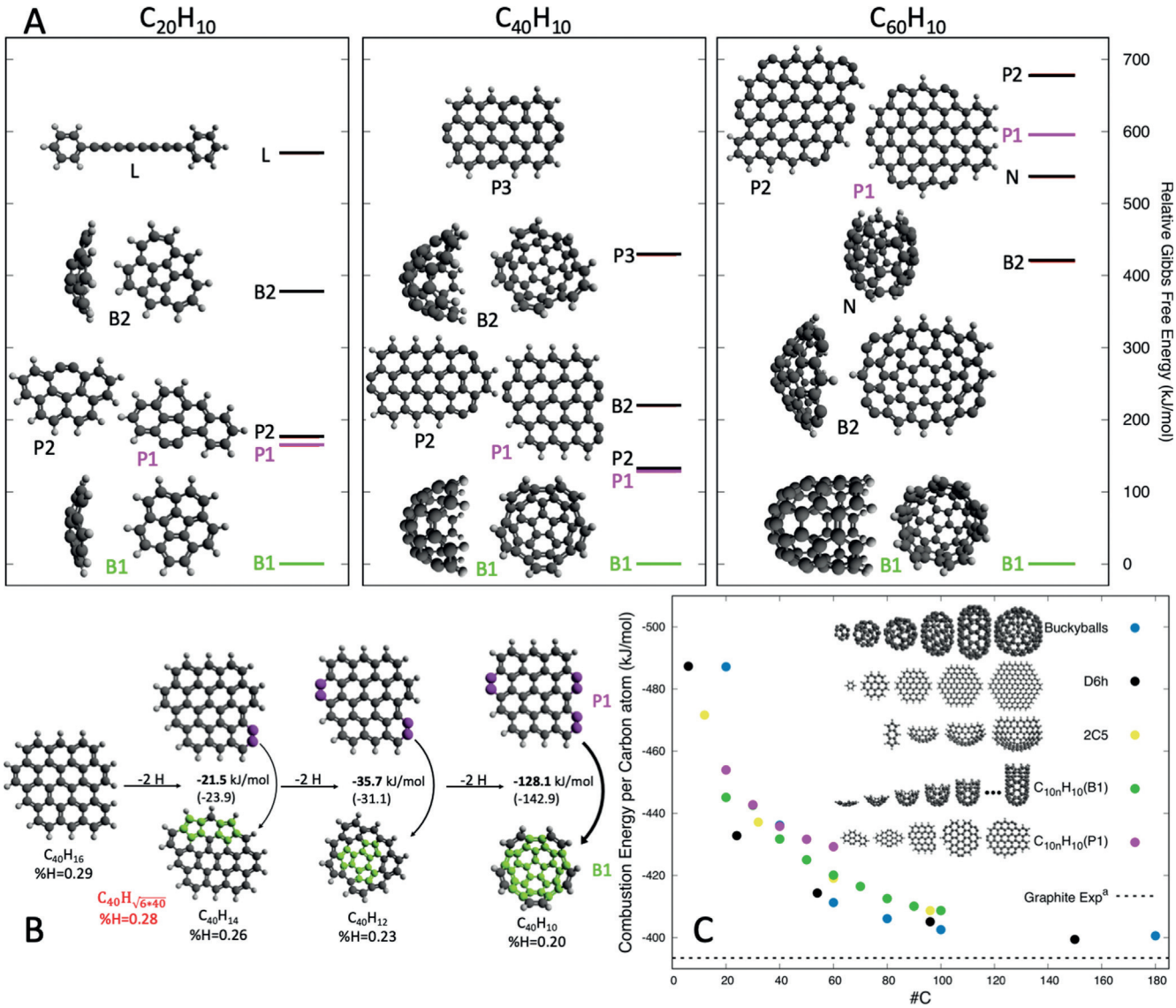

Figure 5. A) relative Gibbs free energies of $C_{20}H_{10}$, $C_{40}H_{10}$, and $C_{60}H_{10}$ obtained at the PBE-D3/DLPNO-CCSD(T) level of theory (see the Supporting Information for computational details). P = planar, B = bowl-shape, N = nanotubes. and L = linear structures. B) Relative stability of planar hydrogen-deficient (magenta) and curved/bowl-shaped structures with 5-membered rings (green) of $C_{40}H_{14}$, $C_{40}H_{12}$ and $C_{40}H_{10}$ (DLPNO-CCSD(T), PBE-D3 in parentheses), including the hydrogen percentage compared to that of $C_xH_{\sqrt{6x}}$ for $x = 40$ (red). C) computational combustion energies per carbon atom of: buckyballs, D_{6h} planar structures, 2C5 (structures with two 5-membered rings), bowl-shaped structures $C_{10n}H_{10}$ (B1) with n from 2 to 10, defective planar structures $C_{10n}H_{10}$ (P1) with n from 2 to 6 (PBE-D3, along with the experimental combustion enthalpy of graphene (see the Supporting Information for details).

 © 2020 The Authors. Published by Wiley-VCH Verlag GmbH & Co. KGaA, Weinheim

Table 1: Relevant patterns that can be considered as building blocks of the PAHs in the $C_{10n}H_{10}$ series, as well as their potential geometric and electronic structure.

Structural patterns	Geometric property	Electronic properties
Aromatic 6-membered ring (AR)	Planar	Very stable aromatic pattern, closed shell
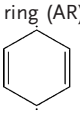 Hydrogen vacancy at zig-zag edges (2C ZZ)	Planar	Not aromatic, open shell (singlet, triplet...)
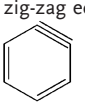 Hydrogen vacancy at armchair edges (C_2 AC)	Planar Distorted C—C triple bond	Not aromatic, closed shell
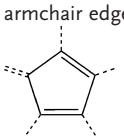 5-membered ring (5C)	Induces a 30° angle per 5-membered ring	Not aromatic, can induce closed or open shell structure
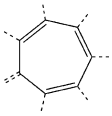 7-membered ring (7C)	Induces a bent structure	Not aromatic, can induce closed or open shell structure
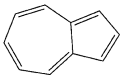 5- and 7-membered rings	Induces an almost planar structure	Not aromatic, can induce closed or open shell structure
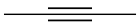 Linear C—C triple bond (C_2L)	Linear	Conjugated, closed shell

cannot only be attributed to the difference in the number of ARs, since they are distinguished by very different "defects", namely a 5-membered ring and hydrogen deficiency at an armchair edge. The other defects introduced in the $C_{20}H_{10}$ series (nanotube, 5- and 7-membered ring combinations, and linear alkynes) are all calculated to lead to structures more than 300 kJ mol^{-1} higher in energy than B1.

The $C_{40}H_{10}$ series is an interesting case, since three structures have the same number of ARs, in this case 10 ARs per structure, thus indicating one bowl structure with six 5-membered rings (B1) and two planar structures (P1 and P2) with 3 hydrogen deficiencies at an armchair edge. The latter are calculated to be about 130 kJ mol^{-1} higher in energy than B1, which is the structure that was found to be lowest in energy in this series. Thus, the results show that 5-membered rings are energetically favourable defects compared to hydrogen-deficient armchair edges. We also considered hydrogen deficiencies at the zig-zag edge (which results in carbenes), as for instance for P3 in the $C_{40}H_{10}$ series, and found that this defect leads to even less stable structures compared to those with only hydrogen deficiency at an armchair edge. Furthermore, as the number of carbon atoms increases, armchair edges will exhibit more hydrogen deficiency defects to retain a planar structure. This leads to a decrease in the number of ARs compared to the bowl structures, thus further increasing their difference in energy, as can be seen for the $C_{60}H_{10}$ series. Overall, the calculations indicate that for the $C_{10n}H_{10}$ series, bowl-shaped structures including 5-membered rings are generally more stable than planar structures. As the size of the system increases, our calculations show that hydrogen-deficient flat structures will be less stable compared to the non-planar ones.

In fact, any polyaromatic hydrocarbon (PAH) core with hydrogen content larger or equal to that of $C_xH_{\sqrt{6x}}$ is likely to have a planar structure. However, compounds with lower hydrogen percentage, such as members of the $C_{10n}H_{10}$, series will incorporate 5-membered ring(s) rather than having hydrogen-deficient edges (see Figure 5B). This is due to the high energy penalty of hydrogen-termination defects compared to the incorporation of 5-membered rings. Hence, the lower the hydrogen content, the higher the number of 5-membered rings can be; for the fullerene-related structures studied here, up to 12. The line in Figure 2B represents the real planar limit, above which compounds have to be considered as non-planar, while the ones below can be planar depending on the length of aliphatic side chains.

A comparison of the thermodynamic stability across different structural motifs (Figure 5C) confirms this trend. While ultimately, and not surprisingly, the ideal graphitic flat structures are the most stable ones (black dots), spherical (blue dots) and bowl-shaped (green dots) structures will be favorable compared to planar, defective structures (magenta dots) in the hydrogen deficient-stoichiometries. While it is shown here that fullerenes are present in asphaltenes, the presence of the $C_{10n}H_{10}$ series also lets us formulate a hypothesis on how they might be gradually formed from smaller hydrocarbons. As shown in Figure 6, the different building blocks detected here ($C_{10n}H_{10}$ series) fit perfectly into the structure of some of the different fullerenes.

While these are not quantitative data, the signal with the highest intensity in the mass spectrum in Figure 1, is not C_{60} as could be expected, but a series consisting of C_{40}, C_{42}, and C_{44}. Among the most stable isomers of C_{40}, the one with D_{5d}

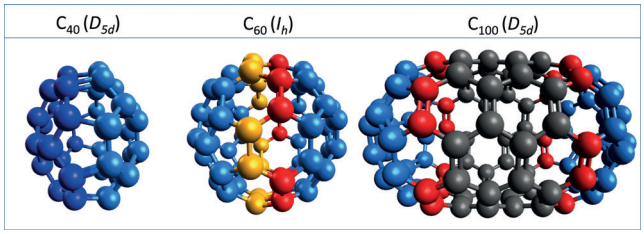

Figure 6. Structural details of some different fullerenes: C_{40} (D_{5h} symmetry) consists of two C_{20} half shells (shown in different shades of blue), while C_{60} consists of two C_{30} endcaps (two C_{20} moieties shown in blue with additional 10 carbon atoms shown in yellow and red for either side). C_{100} (D_{5d} symmetry) shows two such C_{30} endcaps (shown together in blue and red on both sides) and a ring system (in dark grey) that consist of ten 6-membered rings. This ring system can eventually be expanded in armchair configuration to form larger fullerenes of the same symmetry.

 © 2020 The Authors. Published by Wiley-VCH Verlag GmbH & Co. KGaA, Weinheim

symmetry consists of two fused C_{20} parts, which can be considered as being derived from a building block known as corannulene (see $C_{20}H_{10}$ in Figure 4 and Figure 5). C_{60} consists of two C_{30} endcaps (an extension of the corannulene with ten additional carbon atoms forming five additional cyclopentadiene-rings: see $C_{30}H_{10}$ in Figure 4) that can be found in a large number of fullerenes, with C_{100} (D_{5d} symmetry isomer) being one of them. In the case of C_{100}, the two C_{30} endcaps of C_{60} are connected by an additional ring of ten 6-membered rings.

Conclusion

In contrast to what has been reported, there are not only planar compounds present in crude oil. The results shown here clearly verify that the formation of 5-membered rings within polyaromatic compounds is a suitable way to realize different elemental compositions. The inclusion of 5-membered rings is energetically the most reasonable way to form different types of molecules but in the same time moves the structures away from planar conformation. Here, the formula $C_xH_{\sqrt{6x}}$ is introduced as an excellent approximation for pure aromatic cores as the real planar limit to evaluate the shape, since with a lower hydrogen content, the structures are not planar. Each 5-membered ring adds an angle of 30°, and adding more will finally lead to spherical compounds like fullerenes and their building blocks, buckybowls.

Considering the types of structures shown here, from open-ended buckybowls to larger fullerenes, especially ones with D_{5d} symmetry, these results open up the door to other, even larger fullerenes since the length of the ring defines the length and size of the fullerene. Considering the structure of C_{100} being a small tube with two endcaps, the length of the ring can increase. This indicates that detection of these fullerenes could be the stepping-stone, and we envision the presence of carbon nanotubes (CNT) as part of natural fossil materials.

Acknowledgements

A.A.A. and C.P. would like to acknowledge funding by the BMWi (Project No. PtTM@HGS FKZ 03ET6080C). The authors thank Dr. David Stranz (Sierra Analytics, Modesto, CA, USA) for access to software for MS-data evaluation.

Conflict of interest

The authors declare no conflict of interest.

Keywords: buckybowls · coupled-cluster calculations · crude oil · fullerenes · high-resolution mass spectrometry

[1] E. Osawa, *Kagaku* **1970**, *25*, 854 – 863.
[2] H. W. Kroto, J. R. Heath, S. C. O'Brien, R. F. Curl, R. E. Smalley, *Nature* **1985**, *318*, 162 – 163.
[3] a) W. Andreoni, A. Curioni, K. Holczer, K. Prassides, M. KeshavarzK, J. C. Hummelen, F. Wudl, *J. Am. Chem. Soc.* **1996**, *118*, 11335 – 11336; b) W. Krätschmer, L. D. Lamb, K. Fostiropoulos, D. R. Huffman, *Nature* **1990**, *347*, 354 – 358; c) N. Kurita, K. Kobayashi, H. Kumahora, K. Tago, K. Ozawa, *J. Phys. Soc. Jpn.* **1993**, *62*, 2279 – 2284.
[4] a) P. R. Buseck, *Earth Planet. Sci. Lett.* **2002**, *203*, 781 – 792; b) T. J. Millar, *Mon. Not. R. Astron. Soc.* **1992**, *259*, P35 – P39.
[5] a) H. W. Kroto, *Nature* **1987**, *329*, 529 – 531; b) W. Thiel, *Chimia* **1994**, *48*, 447 – 448; c) Z. F. Chen, H. J. Jiao, M. Buhl, A. Hirsch, W. Thiel, *Theor. Chem. Acc.* **2001**, *106*, 352 – 363.
[6] J. Beens, J. Blomberg, P. J. Schoenmakers, *J. High Resolut. Chromatogr.* **2000**, *23*, 182 – 188.
[7] a) A. Gaspar, E. Zellermann, S. Lababidi, J. Reece, W. Schrader, *Anal. Chem.* **2012**, *84*, 5257 – 5267; b) Y. Cho, A. Ahmed, A. Islam, S. Kim, *Mass Spectrom. Rev.* **2015**, *34*, 248 – 263; c) D. S. Pinkston, P. Duan, V. A. Gallardo, S. C. Habicht, X. Tan, K. Qian, M. Gray, K. Mullen, H. I. Kenttamaa, *Energy Fuels* **2009**, *23*, 5564 – 5570; d) D. Borton, D. S. Pinkston, M. R. Hurt, X. L. Tan, K. Azyat, A. Scherer, R. Tykwinski, M. Gray, K. N. Qian, H. I. Kenttamaa, *Energy Fuels* **2010**, *24*, 5548 – 5559.
[8] a) A. G. Marshall, R. P. Rodgers, *Proc. Natl. Acad. Sci. USA* **2008**, *105*, 18090 – 18095; b) J. V. Headley, K. M. Peru, M. P. Barrow, *Mass Spectrom. Rev.* **2016**, *35*, 311 – 328; c) S. K. Panda, J. T. Andersson, W. Schrader, *Angew. Chem. Int. Ed.* **2009**, *48*, 1788 – 1791; *Angew. Chem.* **2009**, *121*, 1820 – 1823; d) A. Vetere, D. Profrock, W. Schrader, *Angew. Chem. Int. Ed.* **2017**, *56*, 10933 – 10937; *Angew. Chem.* **2017**, *129*, 11073 – 11077.
[9] a) A. Gaspar, W. Schrader, *Rapid Commun. Mass Spectrom.* **2012**, *26*, 1047 – 1052; b) Y. J. Cho, J. G. Na, N. S. Nho, S. Kim, S. Kim, *Energy Fuels* **2012**, *26*, 2558 – 2565.
[10] a) A. Vetere, W. Schrader, *ChemistrySelect* **2017**, *2*, 849 – 853; b) D. C. Palacio Lozano, R. Gavard, J. P. Arenas-Diaz, M. J. Thomas, D. D. Stranz, E. Mejía-Ospino, A. Guzman, S. E. F. Spencer, D. Rossell, M. P. Barrow, *Chem. Sci.* **2019**, *10*, 6966 – 6978; c) C. P. Rüger, M. Sklorz, T. Schwemer, R. Zimmermann, *Anal. Bioanal. Chem.* **2015**, *407*, 5923 – 5937; d) C. P. Rüger, C. Grimmer, M. Sklorz, A. Neumann, T. Streibel, R. Zimmermann, *Energy Fuels* **2018**, *32*, 2699 – 2711.
[11] a) M. W. Alachraf, R. C. Wende, S. M. M. Schuler, P. R. Schreiner, W. Schrader, *Chem. Eur. J.* **2015**, *21*, 16203 – 16208; b) A. Vetere, W. Alachraf, S. K. Panda, J. T. Andersson, W. Schrader, *Rapid Commun. Mass Spectrom.* **2018**, *32*, 2141 – 2151.
[12] T. M. C. Pereira, G. Vanini, L. V. Tose, F. M. R. Cardoso, F. P. Fleming, P. T. V. Rosa, C. J. Thompson, E. V. R. Castro, B. G. Vaz, W. Romao, *Fuel* **2014**, *131*, 49 – 58.
[13] M. G. Ikonomou, A. T. Blades, P. Kebarle, *Anal. Chem.* **1991**, *63*, 1989 – 1998.
[14] a) L. Molnárné Guricza, W. Schrader, *J. Mass Spectrom.* **2015**, *50*, 549 – 557; b) G. J. Van Berkel, S. A. McLuckey, G. L. Glish, *Anal. Chem.* **1992**, *64*, 1586 – 1593; c) A. T. Blades, M. G. Ikonomou, P. Kebarle, *Anal. Chem.* **1991**, *63*, 2109 – 2114.
[15] a) R. J. Doyle, M. M. Ross, *J. Phys. Chem.* **1991**, *95*, 4954 – 4956; b) A. B. Young, L. M. Cousins, A. G. Harrison, *Rapid Commun. Mass Spectrom.* **1991**, *5*, 226 – 229; c) R. J. Cotter, *J. Am. Soc. Mass Spectrom.* **2013**, *24*, 657 – 674.
[16] a) S. Grimme, J. Antony, S. Ehrlich, H. Krieg, *J. Chem. Phys.* **2010**, *132*, 154104; b) A. Karton, *J. Comput. Chem.* **2017**, *38*, 370 – 382; c) F. Neese, *Wiley Interdiscip. Rev.: Comput. Mol. Sci.* **2012**, *2*, 73 – 78; d) D. G. Liakos, F. Neese, *J. Chem. Theory Comput.* **2015**, *11*, 4054 – 4063.

Manuscript received: April 14, 2020
Revised manuscript received: May 11, 2020
Accepted manuscript online: May 19, 2020
Version of record online: June 17, 2020

 © 2020 The Authors. Published by Wiley-VCH Verlag GmbH & Co. KGaA, Weinheim